

Supplement of *Clim. Past*, 16, 2039–2054, 2020
<https://doi.org/10.5194/cp-16-2039-2020-supplement>
© Author(s) 2020. This work is distributed under
the Creative Commons Attribution 4.0 License.



Supplement of

Climate simulations and pollen data reveal the distribution and connectivity of temperate tree populations in eastern Asia during the Last Glacial Maximum

Suzanne Alice Ghislaine Leroy et al.

Correspondence to: Klaus Arpe (klaus.arpe@mpimet.mpg.de), and Suzanne Alice Ghislaine Leroy (leroy@msh.univ-aix.fr)

The copyright of individual parts of the supplement might differ from the CC BY 4.0 License.

1
2
3
4
5
6
7
8
9
10
11
12
13
14
15
16
17
18
19
20
21

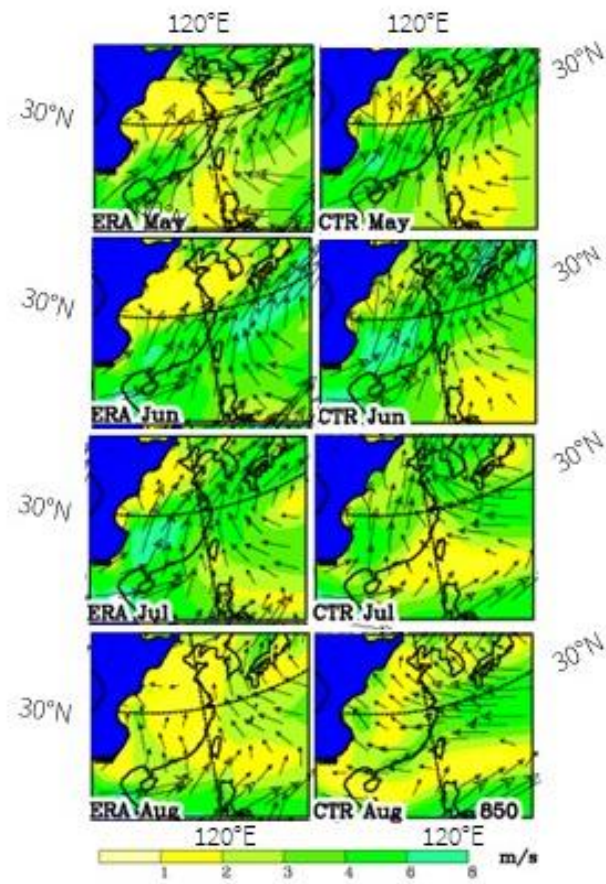
Supporting Information

Supporting Information S1: Monsoon progression in the model compared to observation and

Supporting Information S2: Uncertainty of precipitation analysis

Supporting Information S1: Monsoon progression in the model compared to observation

The climatology of Eastern Asia is dominated by the monsoon. In Fig. S1.1 the winds at the 850 hPa level (around 1500 m height) are displayed for May to August as analysed (ERA) and simulated for the present (CTR). Although the wind is not a limiting factor for tree growth, it has to be considered because of the vital impact of the monsoon precipitation on the climate of Eastern Asia and because of medium to long-distance pollen transport. Comparing ERA with CTR, one can judge the quality of the model used to reproduce the monsoon. Both fields have very similar patterns over the continent in direction and speed, though with a bias to slightly higher speeds in CTR in spring. The differences hardly exceed 1 m/s, except in August over the sea. Because of the good reproduction of the monsoon wind by the model, it is to be expected also that the monsoon for the LGM has been reasonably simulated.



22

23 Fig. S1.1: Wind vectors at 850 hPa over Eastern Asia as analyzed by ERA and as simulated for the
 24 present (CTR) for May to August. Arrows give direction and amplitude of the mean wind and
 25 contours provide the amplitude of the wind vectors. Areas where the 850hPa level lies below
 26 ground are masked.

27

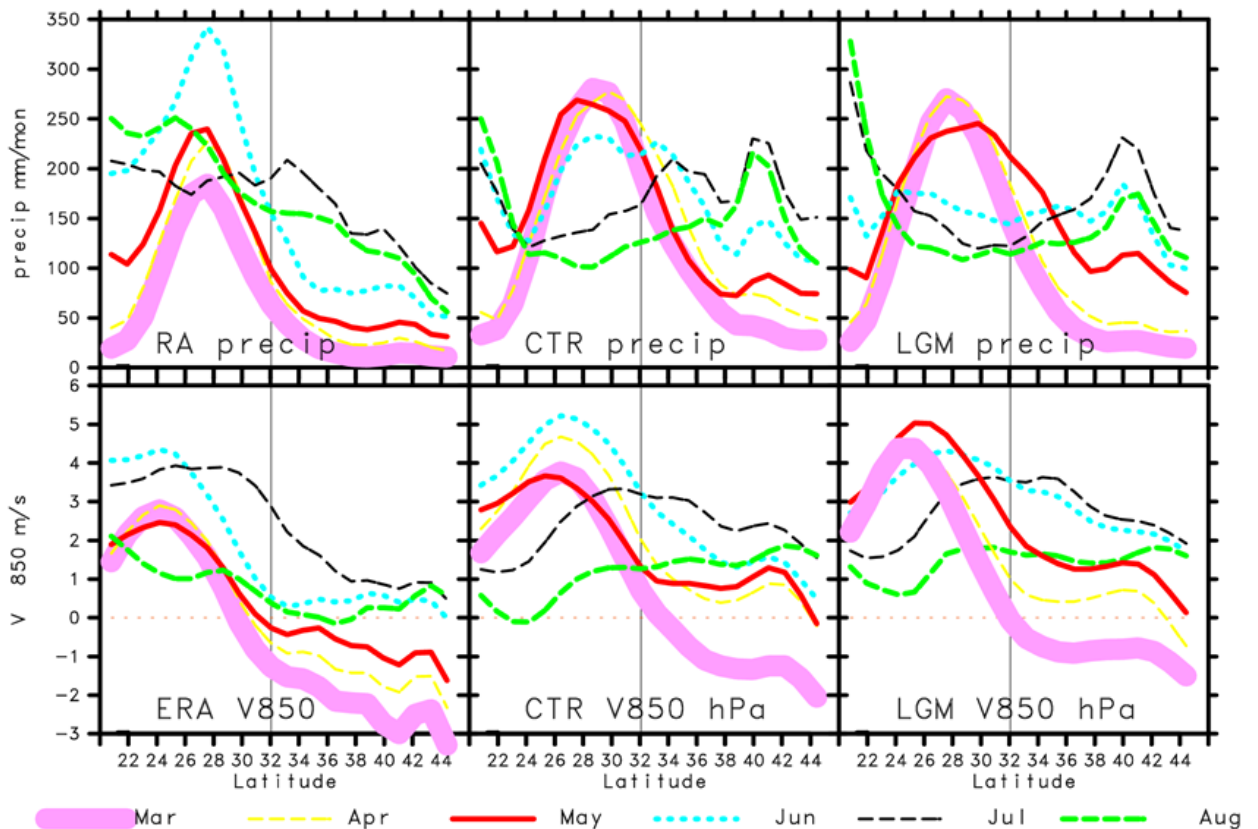
28 The time change of the monsoon wind through spring and summer is further investigated by
 29 comparing the monthly changes of meridional profiles of precipitation and 850hPa meridional
 30 wind averaged between 115 and 119 °E for ERA, CTR and LGM (Fig. S1.2). During spring up to
 31 May the southerly wind in ERA is confined to south of the Qin mountains (32°N), increasing its
 32 speed towards summer and creating there strong precipitation. Then in July the southerlies move
 33 northward to 36°N, another mountain range, spreading the precipitation to there. The 32 °N line is
 34 marked for its importance between the northern and southern China climate which is crossed after
 35 June by the monsoon front. In August, the profiles change completely with stronger southerlies and
 36 precipitation mainly in the northern part.

37 In the CTR simulation, one finds a similar sequence except that the northward propagation of the
 38 monsoon front starts already in June and that a maximum summer precipitation belt occurs on the
 39 southern slope of the mountain range north of 42 °N which can be seen as well in Fig. 4 where this

40 larger precipitation is shown to be an overestimate compared to all climate estimates of the present
 41 precipitation.

42 Comparing CTR and LGM, one finds a general agreement of the monsoon front progression
 43 between the LGM and the CTR simulation, except that for the LGM the monsoon front, also
 44 measured by precipitation, is already moving northward in June while this earlier progression of
 45 the front for CTR is evident only in the wind field. During the LGM this enhanced movement is
 46 also connected with a general decrease of precipitation especially in June and less strong in July.
 47 This leads to a belt of reduced precipitation in summer at 30 to 35 °N for the LGM (Fig. 5).

48
 49



50
 51 *Fig. S1.2: Meridional profiles of precipitation and 850hPa meridional wind averaged between 115*
 52 *and 119°E from 20 to 50°N for ERA, CTR and LGM for March to August. The 32°N line is marked*
 53 *because of its importance between northern and southern China climate.*

54
 55
 56
 57
 58
 59

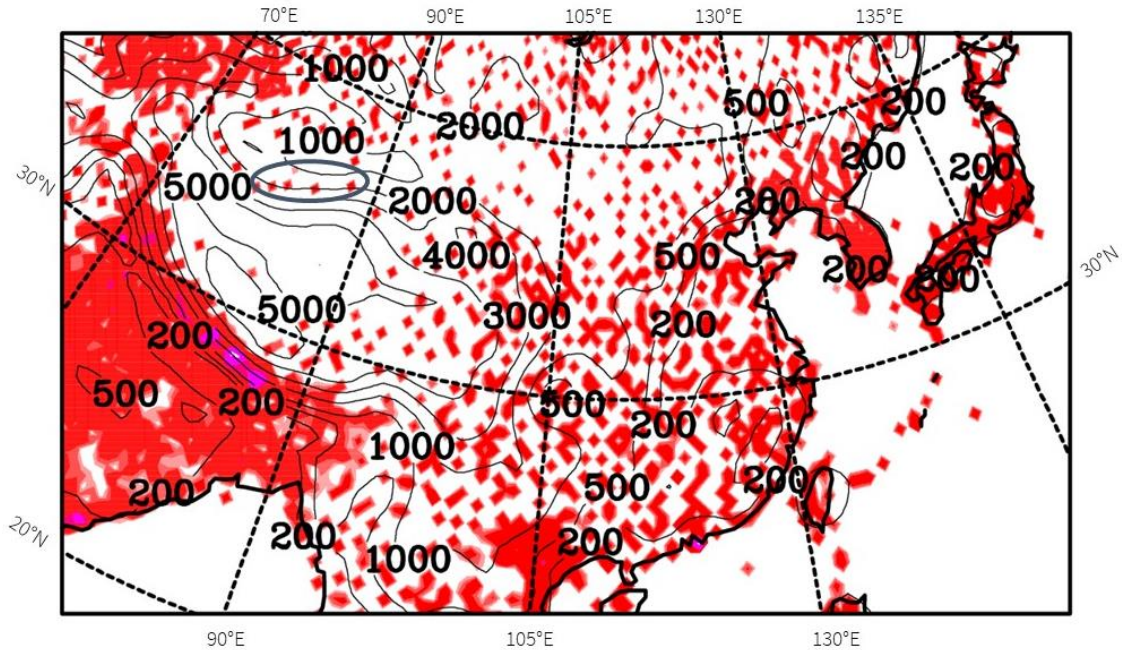
60 **Supporting Information S2: Uncertainty of precipitation analysis**

61

62 In Fig. 4 large differences of precipitation in different climatologies are shown. They are especially
 63 large over the Tibetan Highland. One reason is the low density of observations there (Fig. S2.3).
 64 There are hardly any sites in a large area 30 to 35°N and 80 to 90E° for which all suggest high
 65 precipitation amounts though with considerable differences (Fig. 4). For this study these

66 differences are not important but further north (indicated by an oval in Fig. S2.3) differences are
67 important for the estimate of possible tree growth (Fig. 6 upper panel indicated by ovals).

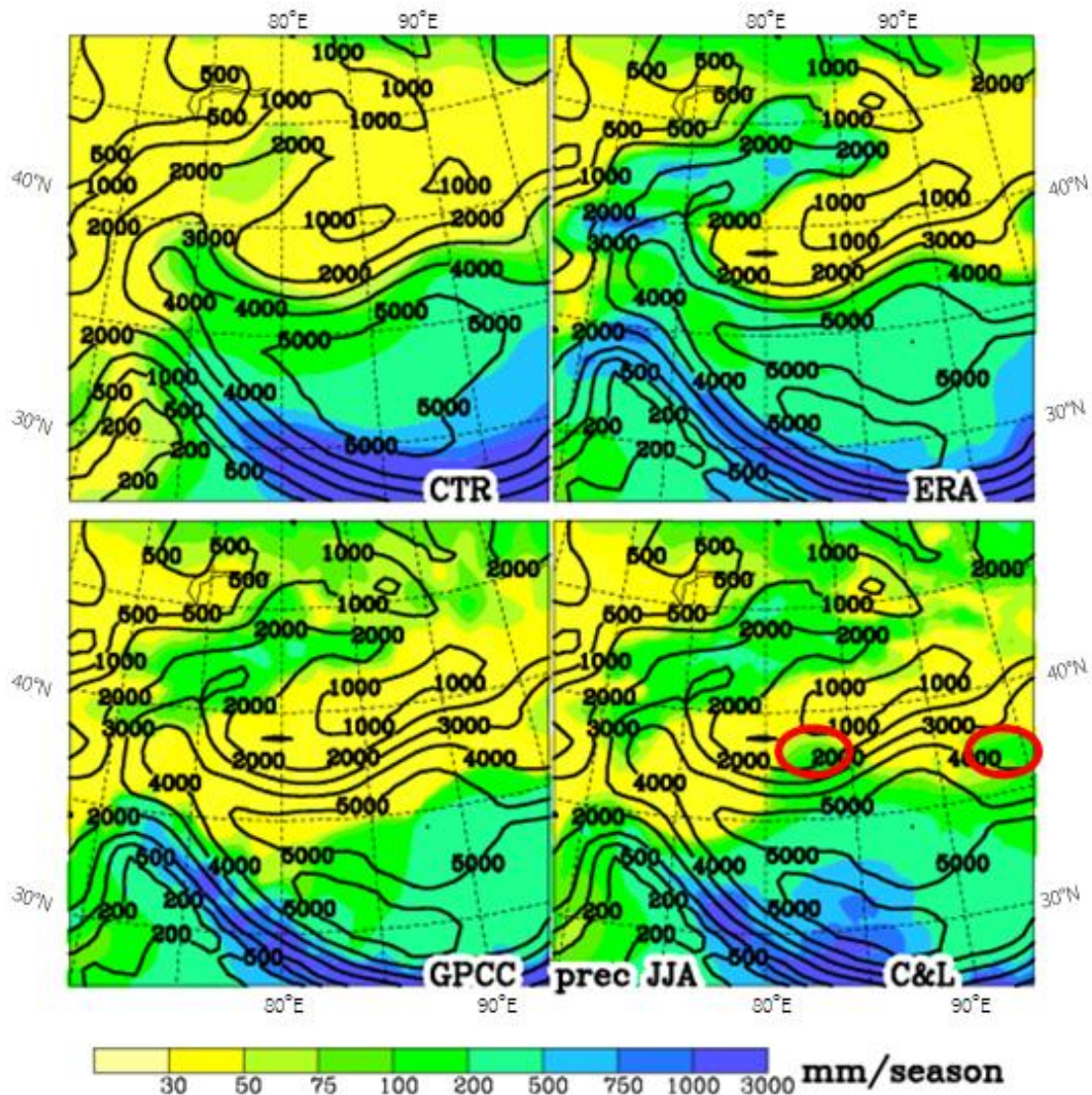
68
69



70
71
72
73
74
75
76

Fig. S2.3: Station density in the GPCC analysis for the season JJA. Dots indicate least one monthly means precipitation observation on average was available each month in a 0.5° grid (blue: more than 3). Black contours give the topography at levels 200, 500, 1000, 2000, 3000, 4000 and 5000 m. The oval in the NE of China indicates where important differences of precipitation from different sources are found.

77 These areas are on the northern slope of the Tibetan Plateau (Fig. S2.4). The distribution of
78 precipitation in the area is very strongly correlated with the topography, low precipitation at lower
79 levels and high precipitation at higher levels along the mountain slopes. All estimates agree in this
80 respect and in the desert valley with topography lower than 2000 m the summer precipitation
81 amounts are below 50 mm/season. Only in the Leemans, R. and Cramer (1991) (C&L)
82 climatology, the contours of precipitation do not follow the contours of the topography on the
83 northern slopes of the Tibetan plateau, the precipitation and topographic contours are almost out of
84 phase in the east-west direction and this results in two erroneous areas of possible tree growth (Fig.
85 6). Because of the low station density in this area (Fig. S2.3), wrong coordinate of a single station
86 can cause large errors. Moreover, the strong orographic structure should be associated with strong
87 spatial variations in precipitation, especially in the north-south direction with a steep slope towards
88 the Tibetan highland, thus strongly reducing the representability of individual station data for a
89 larger domain. Further south (30 °N) of this area one finds another strong deviation of the C&L
90 precipitation climatology from the other ones which is however not important for the present study
91 and not further investigated. ~~Similar climatologies from the Climate Research Unit in East Anglia-~~
92 ~~(CRU, 2016) have a distribution similar to that of GPCC (not shown).~~ We regard these areas of
93 possible tree growth as erroneous. Nevertheless we still regard the C&L climatology very suitable
94 for our purpose.



96

97

98

Fig. S2.4: In colour the climatological precipitation distribution by different data sets and as solid lines the contours of the topography. The circles mark the area where in Fig. 6 possible tree growth was indicated.

99

100

101

102

103

104

When using the ERA data instead of C&L for creating a plot like Fig. 6 (not shown), the unrealistic areas for possible tree growth disappear. This might partly also be due to strong small-scale topographic structures of which the impact from local climates might not be represented by the climatological estimate on a 0.5° grid used here. For Europe this was found at south facing slopes of mountain ranges with respect to the temperature.

104